Near-IR emission of Er^{3+} ions in CsCl-Ga-Ge-S glasses excited by visible light

J. Bunton[a], L. Calvez[b], V. Kadan[c], I. Blonskyi[c], O. Shpotyuk[d,e,f], R. Golovchak[a,*]

[a] *Department of Physics and Astronomy, Austin Peay State University, Clarksville, TN 37044 USA*
[b] *Equipe Verres et Céramiques, UMR-CNRS 6226, Institut des Sciences Chimiques de Rennes, Université de Rennes 1, 35042 Rennes Cedex FRANCE*
[c] *Department of Photonic Processes, Institute of Physics NAS of Ukraine, 46 Prospekt Nauky, Kyiv 03680 UKRAINE*
[d] *Institute of Physics of Jan Dlugosz University, Czestochowa, PL-42-200 POLAND*
[e] *O.G. Vlokh Institute of Physical Optics, 23, Dragomanov str., Lviv, 79005 UKRAINE*
[f] *Scientific Research Company "Carat", 202, Stryjska str., Lviv, 79031 UKRAINE*

Abstract

Fluorescence of $65GeS_2$-$25Ga_2S_3$-10CsCl glasses doped with Er has been investigated at room and liquid nitrogen temperatures. Strong emission lines at ~1 and ~1.5 μm are observed at room temperature in Er-doped samples when excited with ~530 nm wavelength. At cryogenic temperature, this fluorescence is observed even at lower excitation wavelengths (~400-450 nm). The other observed emission and absorption lines agree well with known energy levels transitions of Er^{3+} ions incorporated in the glass matrix and temperature behavior of absorption spectra. The difference between room and liquid nitrogen temperature up-conversion emission is observed under femtosecond pulsed 800 nm laser excitation.

Keywords: fluorescence; chalcogenide glass; rare-earth emission; up-conversion

---

*Corresponding author:
R. Golovchak
e-mail: holovchakr@apsu.edu
Austin Peay State University, 601 College St., Clarksville, TN-37044

1. Introduction

Chalcogenide glasses have been deemed desirable for many applications because of their wide infrared (IR) transmission windows, high refractive indexes, low multiphonon reactions, photo-structural effects, favorable thermal properties and capability to operate at high power, especially at low phonon energy [1,2]. They are easier to synthesize and shape compared to crystalline materials, which makes them more efficient and inexpensive to produce. The combination of these unique properties with good rare-earth solubility also allows the application of chalcogenide glasses in optical sensing, as active media for lasers, optical amplifiers and broad band sources in the mid-IR spectral range, which rely on rare-earth dopant transitions that occur in the high transmission window of the host glass [3-10].

The CsCl-modified Ga-containing germanium sulfide glasses provide one of the best host matrixes for rare-earth elements [4,5]. Their transmission window covers the ~475 nm-12 μm spectral range, where thermal infrared imaging becomes relevant [5,6]. When the alkaline halide CsCl is added to Ga-Ge-S glass stoichiometrically (up to 50 mol.%), the material's optical transmission can be extended further into the short-wave light region up to ~425 nm [7-9]. This drastically increases the possibility for the excitation of rare-earth ions in the glass. Among a variety of rare-earth elements, doping with Er^{3+} ions attracts attention mostly because of $^4I_{13/2} \rightarrow {}^4I_{15/2}$ ground state transition occurring around 1.55 μm – a standard telecommunication wavelength [9]. Typically, Ga-Ge-S glasses will dissolve up to ~1 at. % of Er^{3+} [10], which makes them supreme candidates for IR optical fibers and waveguides used in telecommunications [4,5,11].

In this paper, the room and cryogenic temperature fluorescence in CsCl modified Ga-Ge-S glasses doped with Er is studied. The effect of temperature helps to reveal peculiarities of Er^{3+}

transitions in the above glass matrix, which will allow further engineering of these materials and tailoring for specific applications.

2. Experimental

The Er-doped (0.6 and 1.0 at.%) 65GeS$_2$-25Ga$_2$S$_3$-10CsCl glasses were prepared through a standard melt-quench method. Pure raw 5N materials (Ge, Ga, S, CsCl and Er in metallic form) were melted at 890-930 °C in evacuated silica ampoule for 12 hours before being quenched from 850 °C in a cold water. Special purification procedures were used to obtain high purity glass, as described by Masselin, et al [9]. Glasses were annealed at T_g-15°C for 5 hours in order to minimize the mechanical strains produced during the quench. Then, the samples were cut into 1 mm thick disks (8 mm in diameter) and polished for optical measurements.

The fluorescence spectra were measured at room (T_R = 298 K) and liquid nitrogen (T_{LN} = 77 K) temperatures using Horiba Fluorolog-3 spectrofluorimeter equipped with xenon short arc lamp as a light source. The 300-950 nm wavelengths range was used for excitation, while the emission spectra were collected in the 970-1600 nm range using liquid nitrogen cooled Horiba Jobin Yvon InGaAs DSS-IGA020L detector. A special two-layer fused silica glass Dewar assembly (Horiba FL 1013), which is transparent in the visible and infrared regions of spectrum, was used for measurements at cryogenic temperature. The Dewar was filled with liquid nitrogen (LN) and the samples were completely submerged in LN throughout the entire measurement period.

Optical transmission in the fundamental optical absorption region was measured using Avantes AvaSpec spectrometer equipped with a halogen light source. Transmission at cryogenic temperature was recorded using the same fused silica Dewar assembly and immersion of the samples in liquid nitrogen.

The up-conversion fluorescence spectra were measured with Acton SP-2500i spectrograph at room (T_R = 298 K) and liquid nitrogen (T_{LN} = 77 K) temperatures using a Ti-sapphire 800 nm femtosecond laser, Mira Optima 900-F, for excitation. Recorded emission spectra were corrected for the grating efficiency, CCD spectral sensitivity and transmittance of the colored glass filter, used for elimination of the scattered 800 nm light.

3. Results and Discussion

Optical transmission spectra of Er-doped CsCl-Ga-Ge-S glasses at room and LN temperatures are shown in Fig. 1. The same spectra of un-doped glass (insert to Fig. 1) looked featureless in good agreement with other studies [8], which allowed the assignment of the observed absorption bands in Fig. 1 explicitly to the absorption of Er in CsCl-Ga-Ge-S glass matrix. The absorption lines observed at room temperature located at ~491, ~524, ~546, ~658, ~803 and ~981 nm correspond to known Er^{3+} ion transitions identified as $^4I_{15/2} \rightarrow {}^4F_{7/2}$, $^4I_{15/2} \rightarrow {}^2H_{11/2}$, $^4I_{15/2} \rightarrow {}^2S_{3/2}$, $^4I_{15/2} \rightarrow {}^4F_{9/2}$, $^4I_{15/2} \rightarrow {}^4I_{9/2}$ and $^4I_{15/2} \rightarrow {}^4I_{11/2}$, respectively [10,12-15]. The strongest absorption appears at ~524 nm (Fig. 1). The temperature decrease leads to a significant (~30 nm) short-wave shift of the fundamental optical absorption edge for all of the investigated glasses (Fig. 1), which is consistent with known temperature behavior of the optical gap for this class of amorphous materials [16]. All the above absorption lines are observed at LN temperature too; their positions are about the same, but the intensity slightly increases (Fig. 1). At the same time, at LN temperature, an additional absorption band at ~453 nm, not present in room temperature transmission spectra, becomes noticeable. This absorption corresponds to $^4I_{15/2} \rightarrow {}^4F_{3/2}$ transition of Er^{3+} ion [12-15] and has never been observed in chalcogenide matrixes due to its overlap with fundamental optical absorption edge of previously studied compositions. The transition, however, has a significant impact on fluorescence spectra, as can be ascertained from Fig. 2. The observed absorption and emission lines are summarized more concisely in energy level diagram in Fig. 3.

The fluorescent spectra of un-doped and Er-doped CsCl-Ga-Ge-S glasses at room and LN temperatures are shown in Fig. 2. As expected, the un-doped samples do not show any fluorescence neither at room or LN temperatures (Fig. 2a,b). When 0.6 or 1.0 % of Er is introduced into the matrix, the room-temperature fluorescence shows four distinct emission features in 900-1650 nm range, namely bands at ~990, ~1170, ~1250 and ~1550 nm (Fig. 2c,e). The origin of these bands can be understood from the analysis of energy level diagram for Er^{3+} ions in Fig. 3 and excitation spectrum in Fig. 2. From this data, it follows that the excitation wavelengths at which the fluorescence is observed directly correspond to the absorption lines observed in transmission spectra of the investigated Er-doped CsCl-Ga-Ge-S glasses (Fig. 1). Absorbing ~800 nm wavelength light would populate the $^4I_{9/2}$ level of the Er^{3+} ion, which may decay via a multiphonon relaxation mechanism [12] and populate the $^4I_{11/2}$ and $^4I_{13/2}$ levels, resulting in the observed emission at ~990 and 1550 nm (Fig. 2c, e) due to the ground state $^4I_{11/2} \rightarrow {}^4I_{15/2}$ and $^4I_{13/2} \rightarrow {}^4I_{15/2}$ radiative transitions (Fig. 3). The excitation from ~660 nm wavelength light leads to a population of $^4F_{9/2}$ level, which may directly result in the $^4F_{9/2} \rightarrow {}^4I_{13/2}$ radiative transition responsible for the observed emission band at ~1170 nm (Fig. 2c,e), or decay into $^4I_{9/2}$ or $^4I_{11/2}$ states radiatively or non-radiatively. The following ground state $^4I_{11/2} \rightarrow {}^4I_{15/2}$ and $^4I_{13/2} \rightarrow {}^4I_{15/2}$ radiative transitions would also contribute to the emission at ~990 and ~1550 nm (Fig. 2c, e). The excitation with ~490, ~530 and ~550 nm wavelengths results in a population of $^4F_{7/2}$, $^2H_{11/2}$ and $^4S_{3/2}$ levels, respectively.

The decay of the $^4F_{7/2}$ population can produce a cascade of radiative transitions, like $^4F_{7/2} \rightarrow {}^4I_{11/2}$ and $^4I_{11/2} \rightarrow {}^4I_{15/2}$, which are both observed as emission bands at ~990 nm, as well as several other (including non-radiative) transitions, such as those populating levels $^2H_{11/2}$ and $^4S_{3/2}$. The $^2H_{11/2} \rightarrow {}^4I_{9/2}$ radiative transition would have a contribution to the band at ~1550 nm along with $^4I_{13/2} \rightarrow {}^4I_{15/2}$ one. The intermediate level $^4F_{7/2} \rightarrow {}^4I_{9/2}$ and $^4S_{3/2} \rightarrow {}^4I_{11/2}$ transitions would be responsible for the observed emission band at ~1250 nm, and $^4F_{9/2} \rightarrow {}^4I_{13/2}$ for the emission at ~1170 nm according to the energy level diagram of Er^{3+} ions (Fig. 3). Further decay would ultimately lead to the observation of ground state radiative transitions $^4I_{11/2} \rightarrow {}^4I_{15/2}$ and $^4I_{13/2} \rightarrow {}^4I_{15/2}$.

At LN temperature, the pronounced changes in fluorescence efficiency are observed for all near-IR emission bands of Er-doped glasses (Fig. 4), in full agreement with [17]. Some changes are also noticed for a shape of ~1550 nm band (Fig. 4), which fine structure is caused by Stark splitting due to local electric fields at Er^{3+} sites (determined mostly by local symmetry) [4,18]. The collapse of the line at ~1500 nm leads to an apparent narrowing of ~1550 nm band at LN temperature, which is similar to the low-temperature behavior of fluorescence in Er-doped Ge-Ga-S glasses not containing CsCl [17]. A new emission line at ~1100 nm emerges at LN temperature under the excitation of Er-doped CsCl-Ga-Ge-S samples with 450-550 nm light (Fig. 4). This line corresponds to $^2H_{11/2} \rightarrow {}^4I_{11/2}$ radiative transition, usually not observed at room temperature [17]. Simultaneously, the fluorescence stimulated by the light from 400-500 nm range becomes more intense (Fig. 4), which is correlated with the appearance of the absorption band at ~450 nm in optical transmission spectra of the investigated Er-doped CsCl-Ga-Ge-S glasses at LN temperature (Fig. 1). The absorption of such light would populate $^4F_{3/2}$ level of Er^{3+} ion, which can cause strong emission at ~990 nm and ~1550 nm due to the inner shell $^4F_{3/2} \rightarrow {}^4F_{9/2}$ and $^4F_{3/2} \rightarrow {}^4I_{9/2}$ radiative transitions, as well as subsequent ground state $^4I_{11/2} \rightarrow {}^4I_{15/2}$ and $^4I_{13/2} \rightarrow {}^4I_{15/2}$ radiative transitions during further decay.

The investigated Er-doped glasses are suitable for the up-conversion applications when excited with commercially available coherent light sources, such as a Ti-sapphire laser (800 nm emission), for example [19,20]. Although up-conversion processes stimulated by 800 nm light in Er-doped 65GeS$_2$-25Ga$_2$S$_3$-10CsCl glasses at room temperature are already reported [19], the results at cryogenic temperatures are missing. The room temperature up-conversion fluorescence of these glasses under the excitation of 800 nm light from a Ti-sapphire laser source in femtosecond (fs) regime shows similar features to the reported earlier under 800 nm CW laser excitation [19], e.g. bands at ~660 nm, ~550 nm and ~530 nm (Fig. 5a). The absence of higher than ~530 nm up-conversion fluorescence allows us to exclude two-photon absorption processes leading to a population of conduction band and upper levels of Er^{3+} ions. Then, the excited state absorption (ESA) and energy transfer up-conversion (ETU) mechanisms should be considered [19]. The first mechanism relies on the absorption of ~800 nm light and population of $^4I_{9/2}$ level due to $^4I_{15/2} \rightarrow {}^4I_{9/2}$ transition. Relaxation of this excited state would populate the $^4I_{13/2}$ level, which than can be excited again with ~800 nm light, leading to the population of $^4H_{11/2}$ state. Ground state transition from this level $^2H_{11/2} \rightarrow {}^4I_{15/2}$ would result in the observed up-conversion fluorescence at ~530 nm, while decay of this level into $^4S_{3/2}$ and $^4F_{9/2}$ states would cause up-conversion fluorescence emissions at ~550 nm ($^4S_{3/2} \rightarrow {}^4I_{15/2}$ transition) and ~660 nm ($^4F_{9/2} \rightarrow {}^4I_{15/2}$ transition). The second mechanism, ETU processes, relies on the emission of a photon from one Er^{3+} ion in the excited state and absorption of this photon by another Er^{3+} ion. Such emission-reabsorption processes caused by ~800 nm excitation would lead to the population of $^4S_{3/2}$ and $^4F_{9/2}$ states [19]. From the obtained results (Fig. 5a) it can be concluded that the efficiency of ~550 nm up-conversion ($^4S_{3/2}$

$\rightarrow$ $^4I_{15/2}$ transition) is the highest, indicating the population of $^4S_{3/2}$ level is most efficient. With a decrease in temperature, all up-conversion emission bands become more intense (Fig. 5b), except the band at ~530 nm, which disappears completely (Fig. 5b). The latter phenomenon can be explained by a domination of ETU over ESA mechanisms at LN temperature.

5. Conclusions

The analysis of fluorescence stimulated by visible light in Er-doped CsCl-Ga-Ge-S glasses at room and liquid nitrogen temperatures reveals a number of transitions associated with energy levels of Er^{3+} ions. The $^4I_{15/2} \rightarrow {}^4F_{3/2}$ transition becomes active at LN temperature, which results in the absorption band at ~450 nm in the transmission spectra of Er-doped CsCl-Ga-Ge-S glasses. The population of $^4F_{3/2}$ state causes cascade of radiative transitions resulting in fluorescence bands primarily at ~990 and ~1550 nm. An additional band at ~1100 nm is observed at liquid nitrogen temperature under the excitation of Er-doped CsCl-Ga-Ge-S glasses with 450-550 nm light. It is attributed to $^2H_{11/2} \rightarrow {}^4I_{11/2}$ radiative transition, which is not observed at room temperature. So far, the Er-doped CsCl-Ga-Ge-S glasses provide the largest number of possible Er^{3+} transitions among all chalcogenide matrixes, which can be used for up- and down-conversions in photonics. Specifically, the excitation with 800 nm laser pulses of ~fs duration at room temperature results in 3 up-conversion lines at ~530 nm, 550 nm and 660 nm wavelengths. A decrease in temperature causes ~530 nm emission to cease under similar excitation conditions.

Acknoledgments

VK, IB and OS acknowledge support from the STCU-NASU Targeted Initiative Program (Project 6174), NASU-TÜBİTAK joint R&D project, bilateral Ukrainian-French DNIPRO program supported by CAMPUS FRANCE and Ministry of Education and Science of Ukraine (Project 37559QB), as well as from the Ukrainian State Fund for Fundamental Research (Project F73/23805). The group from Austin Peay State University acknowledges NSF Grant DMR-1409160 for the financial support of undergraduate research program in glass science.

References

[1] J-L. Adam, X. Zhang (Eds.), Chalcogenide Glasses: Preparation, properties and application, Woodhead Publishing series in Electronic and Optical Materials No.44, 2014.

[2] A. Seddon, Chalcogenide glasses: a review of their preparation, properties and applications, Journal of Non-Crystalline Solids 184 (1995) 44-50.

[3] D. Marchese, G. Kakarantzas, A. Jha, $^1G_4$ lifetimes, optical and thermal characteristics of Pr-doped GeS_2-chalcohalide glasses, J. Non-Cryst. Solids 196 (1996) 314-319.

[4] M. Munzar, C. Koughia, D. Tonchev, K. Maeda, T. Ikari, C. Haugen, R. Decorby, J. McMullin, S. Kasap, Optical properties of Er-doped $Ga_x(Ge_{0.3}Se_{0.7})_{100-x}$ glasses, Optical Materials 28 (2006) 225-230.

[5] F. Prudenzano, L. Mescia, L. Allegretti, V. Moizan, V. Nazabal, F. Smektala, Theoretical study of cascade laser in erbium-doped chalcogenide glass fibers, Optical Materials 33 (2010) 241-245.

[6] P. Masselin, D. Le Coq, L. Calvez, E. Petracovschi, E. Lepine, E. Bychkov, X. Zhang, CsCl effect on the optical properties of the $80GeS_2$-$20Ga_2S_3$ base glass, Applied Physics A106, *3* (2012) 697-702.

[7] A. Brehault, L. Calvez, P. Adam, J. Rollin, M. Cathelinaud, B. Fan, O. Merdrignac-Conanec, T. Pain, X.-H. Zhang, Moldable multispectral glasses in GeS_2-Ga_2S_3-CsCl system transparent from the visible up to the thermal infrared regions, J. Non-Cryst. Solids 431 (2016) 25-30.

[8] K. Koughia, M. Munzar, D. Tonchev, C. Haugen, R. Decorby, J. McMullin, S. Kasap, Photoluminescence in Er-doped Ge-Ga-Se glasses, J. of Luminescence 112 (2005) 92-96.

[9] P. Masselin, D. Le Coq, L. Calvez, E. Petracovschi, E. Lépine, E. Bychkov, CsCl effect on the optical properties of the $80GeS_2$–$20Ga_2S_3$ base glass, Appl. Phys. A 106 (2012) 697–702.

[10] T. Ivanova, A. Man'shina, A. Povolotskiy, Cross-relaxation processes and structural modifications in Ga-Ge-S:Er^{3+} chalcogenide glasses, J. Non-Cryst. Solids 351 (2005) 1403-1409.

[11] K. Maeda, T. Sakai, D. Tonchev, M. Munzar, T. Ikari, S. Kasap, The influence of Te on thermal properties of Er-doped $(Ge_{30}(Se_{1-x}Te_x)_{70})_{94}Ga_6$ chalcogenide glasses, Materials Science and Engineering B 122 (2005) 20-23.

[12] Z. Pan, A. Ueda, R. Aga, A. Burger, R. Mu, S.H. Morgan, Spectroscopic studies of Er^{3+} doped Ge-Ga-S glass containing silver nanoparticles, J. Non-Cryst. Solids 356 (2010) 1097–1101.

[13] K. Kadono, T. Yazawa, Sh. Jiang, J. Porque, B.-Ch. Hwang, N. Peyghambarian, Rate equation analysis and energy transfer of Er^{3+}-doped Ga_2S_3–GeS_2–La_2S_3 glasses, J. Non-Cryst. Solids 331 (2003) 79–90.

[14] T.Yu. Ivanova, A.A. Man'shina, A.V. Kurochkin, Yu.S. Tver'yanovich, V.B. Smirnov, Er^{3+} to glass matrix energy transfer in Ga–Ge–S:Er^{3+} system, J. Non-Cryst. Solids 298 (2002) 7–14.

[15] T.Yu. Ivanova, A.A. Man'shina, A.V. Kurochkin, Yu.S. Tver'yanovich, V.B. Smirnov, Non-radiative energy transfer from Er^{3+} ions to the electronic states of the chalcogenide glass matrix, J. Non-Cryst. Solids 326&327 (2003) 320–324.

[16] A. Feltz, Amorphous Inorganic Materials and Glasses, VCH, Weinheim, 1993.

[17] Z.G. Ivanova, J. Zavadil, K.S.R.K. Rao, Compositional trends in low-temperature photoluminescence of heavily Er-doped GeS_2–Ga_2S_3 glasses, J. Non-Cryst. Solids 357 (2011) 2443–2446.

[18] V. Seznec, H. Ma, X. Zhang, V. Nazabal, J.-L. Adam, X.S. Qiao, X.P. Fan, Spectroscopic properties of Er^{3+}-doped chalcohalide glass ceramics, Proc. of SPIE 6116 (2006) 61160B-1-9.

[19] R. Balda, S. García-Revilla, J. Fernández. V. Seznec, V. Nazabal, X.H. Zhang, J.L. Adam, M. Allix, G. Matzen, Upconversion luminescence of transparent Er^{3+}-doped chalcohalide glass-ceramics, Optical Materials 31 (2009) 760–764.

[20] Z.G. Ivanova, M. Jayasimhadri, J. Heo, J. Zavadil, Up-conversion fluorescence and low-temperature emission in Er^{3+}-doped GeGaS–CsBr glasses, J. Non-Cryst. Solids 356 (2010) 2393–2396.

Figure captions

Figure 1. Transmission spectra of $65GeS_2$-$25Ga_2S_3$-10CsCl glasses un-doped (insert) and doped (main figures) with 0.6 and 1.0 at.% of Er, recorded at room (T_R) and liquid nitrogen (T_{LN}) temperatures. Indicated wavelengths correspond to Er^{3+} ions absorption.

Figure 2. Fluorescence spectra of $65GeS_2$-$25Ga_2S_3$-10CsCl glasses un-doped (a,b) doped with 0.6 at.% (c,d) and 1.0 at.% (e,f) of Er, recorded at room (a,c,e) and liquid nitrogen (b,d,f) temperatures. Straight (grey) lines are caused by Rayleigh scattering of the excitation light (ignored during analysis). Redistribution of fluorescence intensity is seen at LN temperature.

Figure 3. Energy level diagram for Er^{3+} ion [12,14]. The observed absorption and emission transitions are shown with arrows.

Figure 4. Compared fluorescence spectra (not normalized) of $65GeS_2$-$25Ga_2S_3$-10CsCl glasses doped with 0.6 at.% and 1.0 at.% of Er, recorded at different temperatures and selected excitation wavelengths. Redistribution of fluorescence intensity and new emission lines are observed at cryogenic temperature.

Figure 5. Up-conversion fluorescence of Er^{3+} ions in $65GeS_2$-$25Ga_2S_3$-10CsCl glass matrix, stimulated by 800 nm femtosecond laser pulses at room (a) and LN (b) temperatures. Disappearance of ~530 nm emission line at LN temperature is obvious.

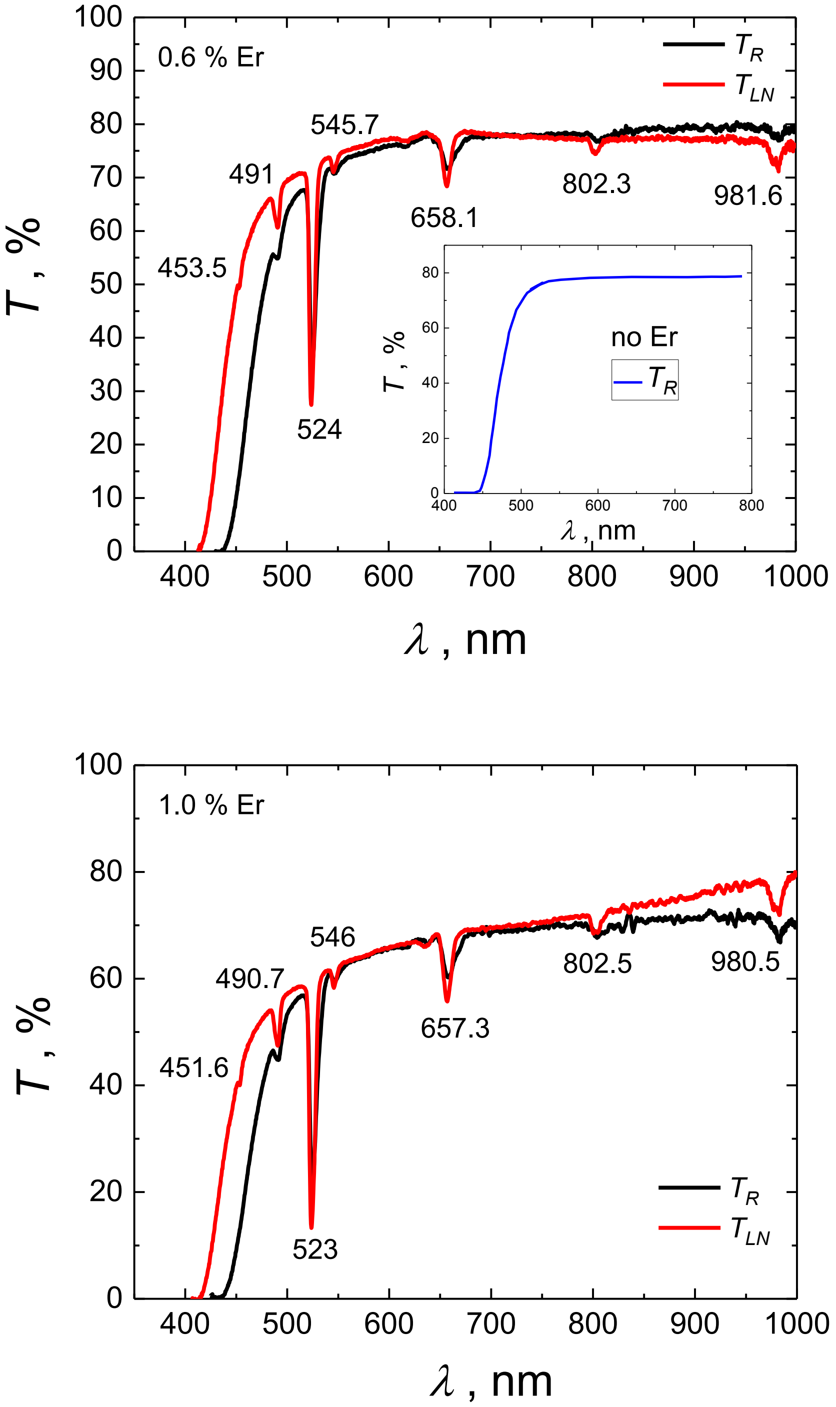
0.6 % Er
T_R
T_{LN}
100
90
80
70
60
50
40
30
20
10
0
T , %
453.5
491
545.7
524
658.1
802.3
981.6
400
500
600
700
800
900
1000
λ , nm
no Er
T_R
T , %
80
60
40
20
0
400
500
600
700
800
λ , nm
1.0 % Er
100
80
60
40
20
0
T , %
451.6
490.7
546
523
657.3
802.5
980.5
T_R
T_{LN}
400
500
600
700
800
900
1000
λ , nm

Fig. 1.

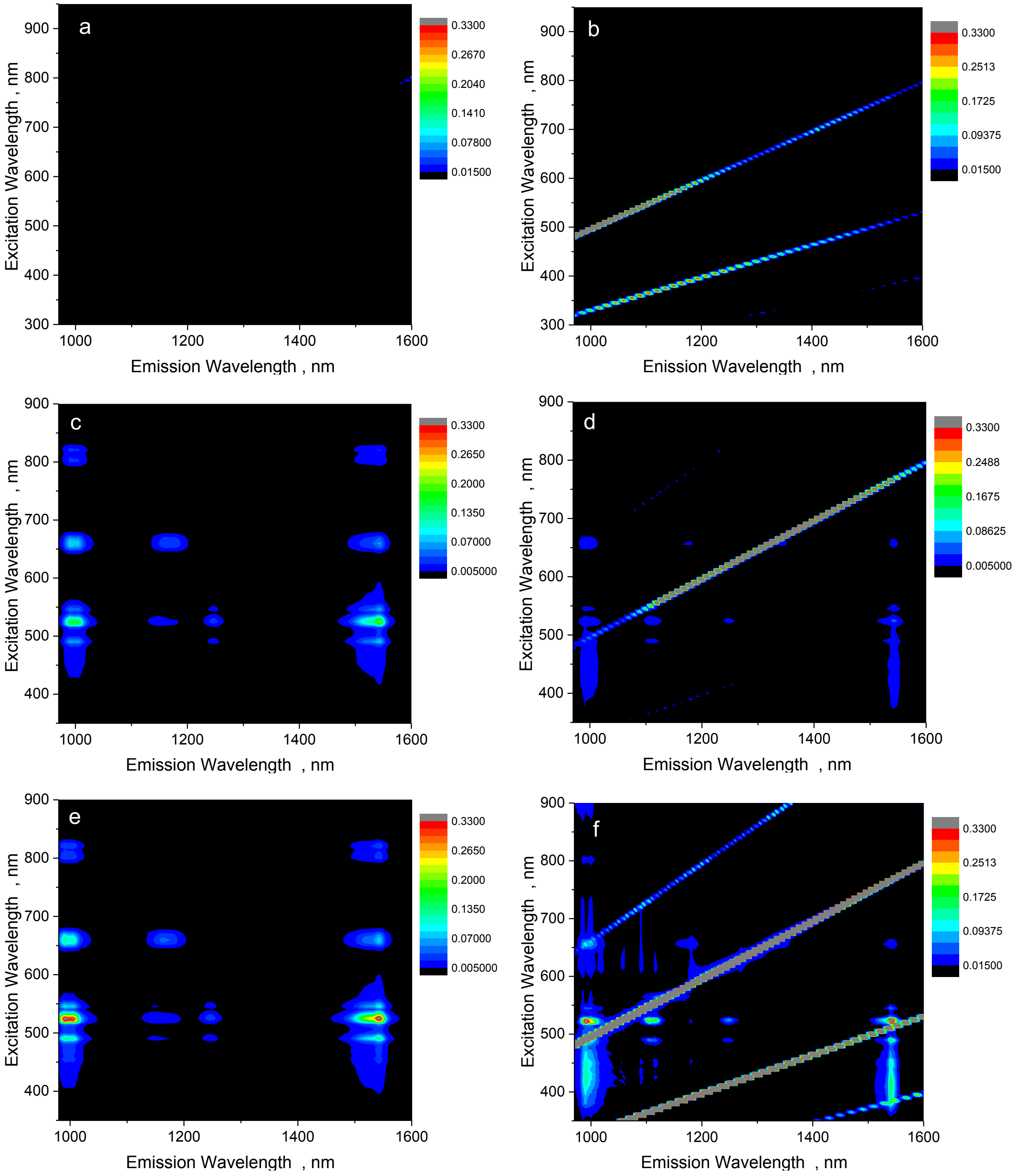
a
b
c
d
e
f
Excitation Wavelength , nm
Emission Wavelength , nm
Enission Wavelength , nm
300
400
500
600
700
800
900
1000
1200
1400
1600
0.3300
0.2670
0.2040
0.1410
0.07800
0.01500
0.2513
0.1725
0.09375
0.2650
0.2000
0.1350
0.07000
0.005000
0.2488
0.1675
0.08625

Fig. 2.

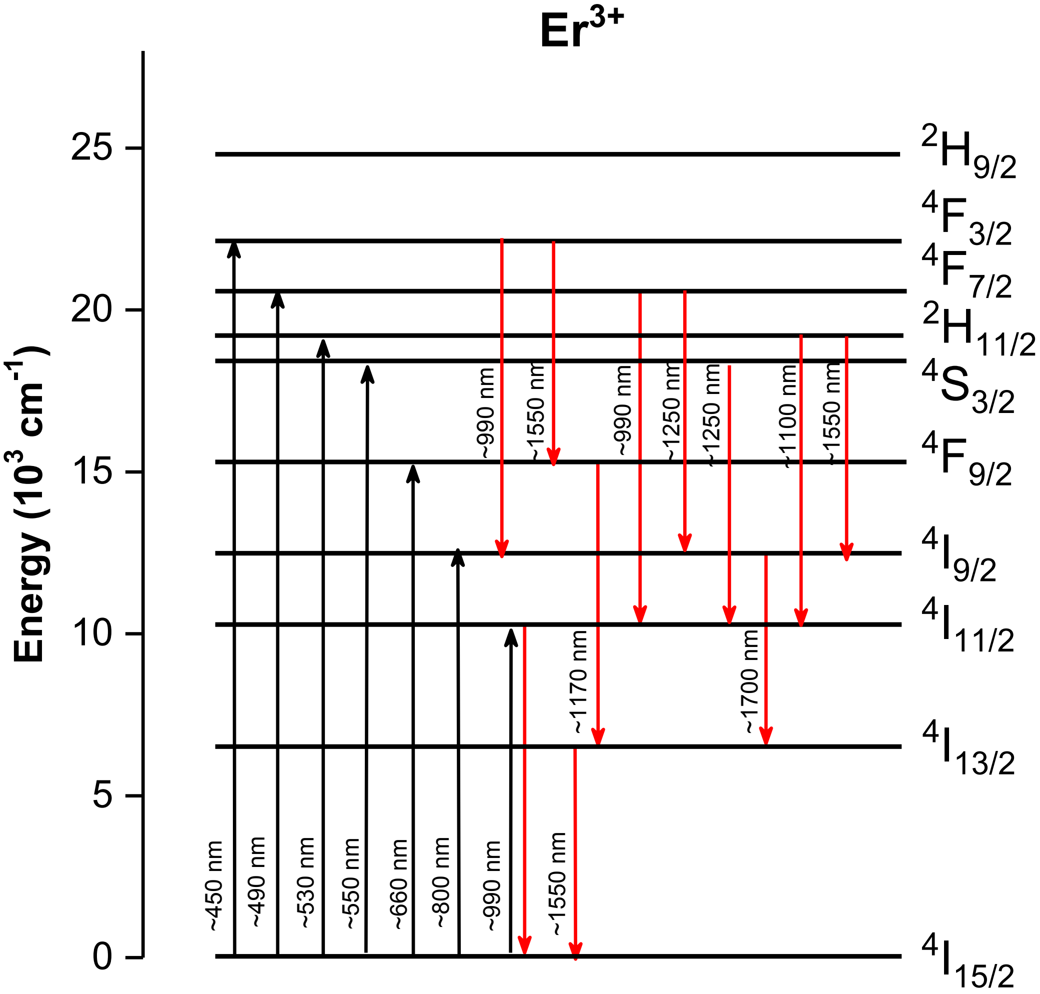
Er^{3+}
Energy (10^3 cm^{-1})
25
20
15
10
5
0
$^2H_{9/2}$
$^4F_{3/2}$
$^4F_{7/2}$
$^2H_{11/2}$
$^4S_{3/2}$
$^4F_{9/2}$
$^4I_{9/2}$
$^4I_{11/2}$
$^4I_{13/2}$
$^4I_{15/2}$
~450 nm
~490 nm
~530 nm
~550 nm
~660 nm
~800 nm
~990 nm
~1550 nm
~990 nm
~1550 nm
~990 nm
~1250 nm
~1250 nm
~1100 nm
~1550 nm
~1170 nm
~1700 nm

Fig. 3.

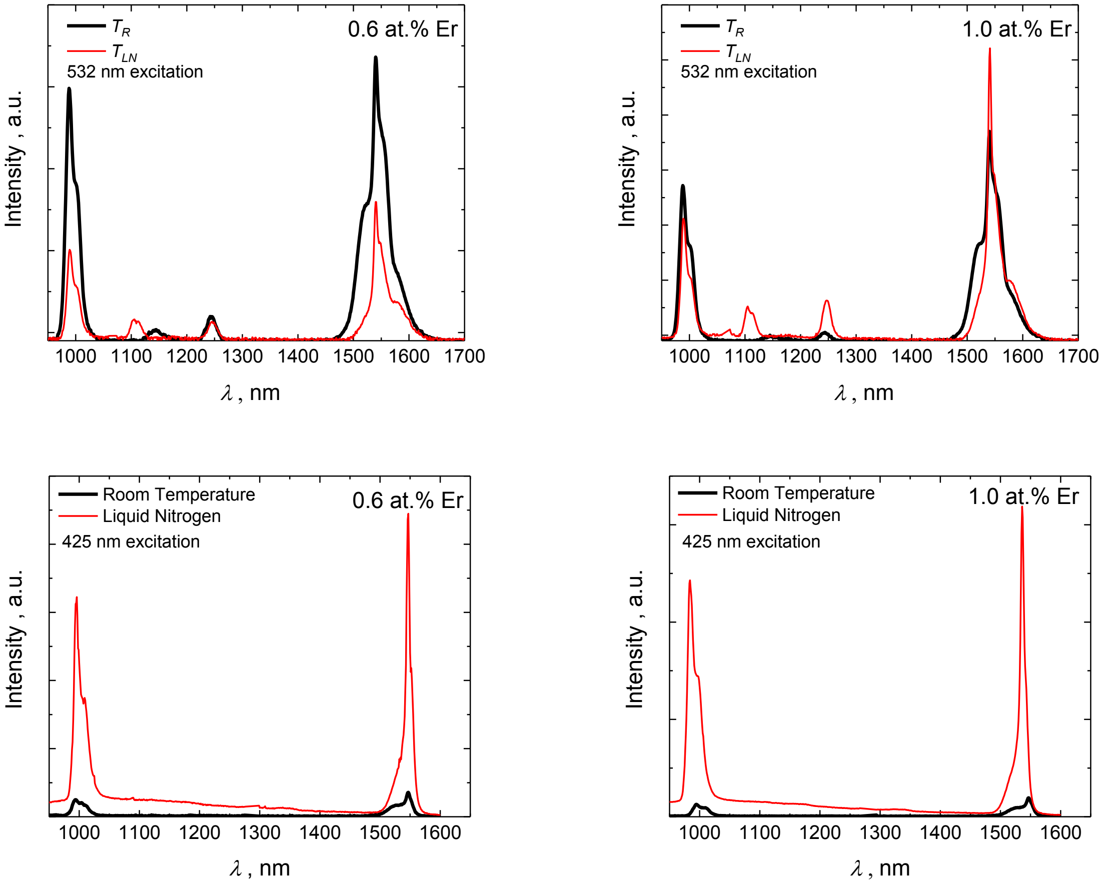

T_R
T_LN
532 nm excitation
0.6 at.% Er
1.0 at.% Er
Room Temperature
Liquid Nitrogen
425 nm excitation
Intensity , a.u.
λ , nm
1000
1100
1200
1300
1400
1500
1600
1700

Fig. 4.

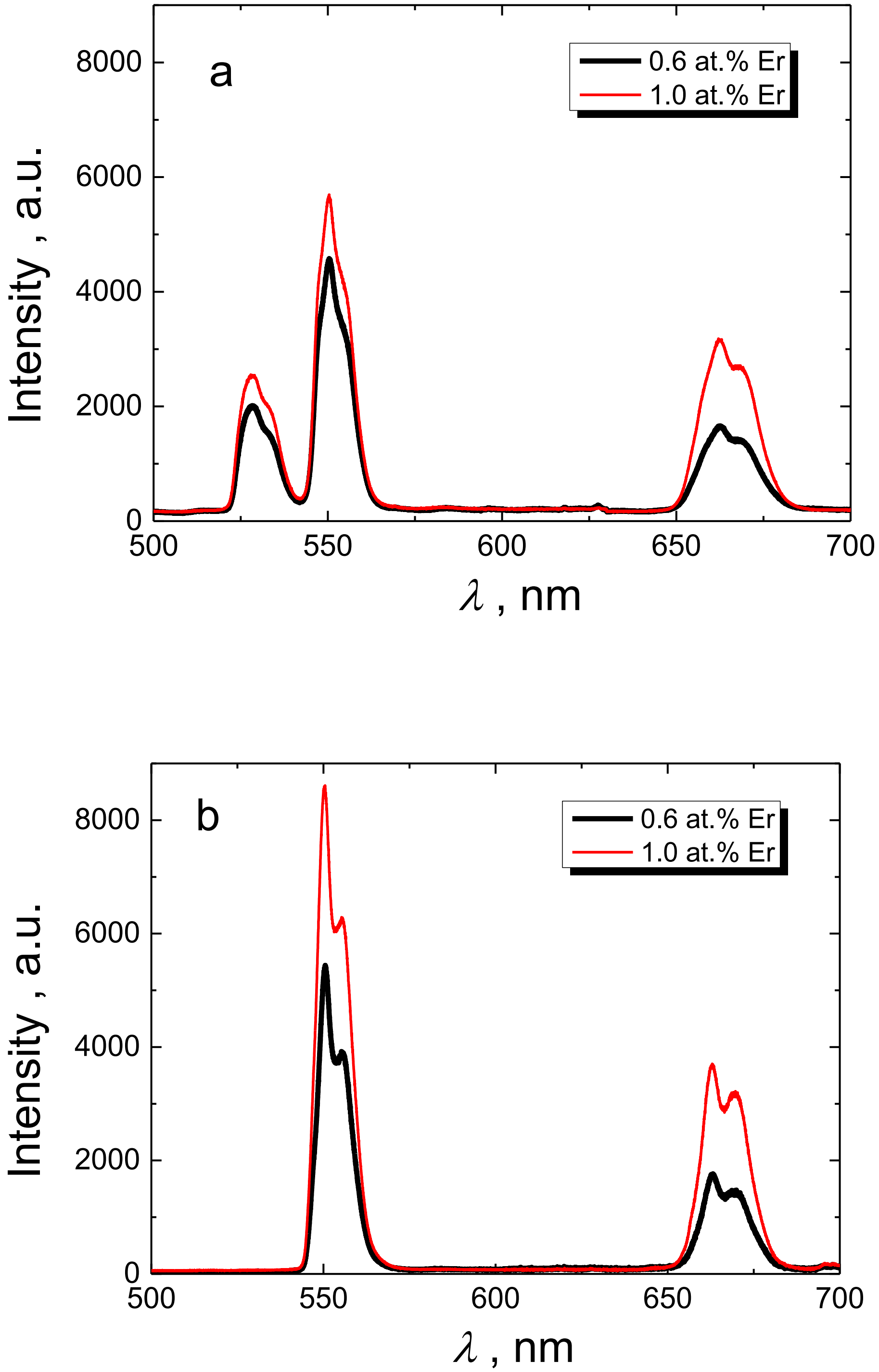
a
0.6 at.% Er
1.0 at.% Er
Intensity , a.u.
0
2000
4000
6000
8000
500
550
600
650
700
λ , nm
b
0.6 at.% Er
1.0 at.% Er
Intensity , a.u.
0
2000
4000
6000
8000
500
550
600
650
700
λ , nm

Fig. 5.